



## Preparation of $\text{Fe}_2\text{O}_3$ modified kaolin and application in heterogeneous electro-catalytic oxidation of enoxacin

Ali Özcan <sup>a,\*</sup>, Ayça Atılır Özcan <sup>a</sup>, Yusuf Demirci <sup>a</sup>, Erol Şener <sup>b</sup>

<sup>a</sup> Anadolu University, Faculty of Science, Department of Chemistry, 26470, Eskisehir, Turkey

<sup>b</sup> Anadolu University, Faculty of Pharmacy, Department of Analytical Chemistry, 26470, Eskisehir, Turkey



### ARTICLE INFO

#### Article history:

Received 13 March 2016

Received in revised form 3 July 2016

Accepted 14 July 2016

Available online 16 July 2016

#### Keywords:

Enoxacin

Electro-Fenton

Iron oxide

Hydroxyl radical

Heterogeneous catalysis

### ABSTRACT

Preparation and use of an iron containing catalyst,  $\text{Fe}_2\text{O}_3$  modified kaolin ( $\text{Fe}_2\text{O}_3$ -KLN), was investigated to develop a heterogeneous electro-Fenton process for the electrochemical oxidation of enoxacin (ENXN). The characterizations of the prepared  $\text{Fe}_2\text{O}_3$ -KLN were performed using different methods. Mineralization efficiency of the electro-Fenton method increased in the presence of  $\text{Fe}_2\text{O}_3$ -KLN catalyst. The experimental variables that affect the efficiency of heterogeneous electro-Fenton treatment were investigated. Mineralization rates of ENXN reached its maximal value in the presence of 0.3 g  $\text{Fe}_2\text{O}_3$ -KLN at 300 mA. While the mineralization efficiency of ENXN was much higher in pH values of 2.0 and 3.0, the total mineralization of ENXN was also observed at pH values of 5.1 and 7.1. A very small decrease (0.5%) was found in the activity of  $\text{Fe}_2\text{O}_3$ -KLN after five runs. Characterization studies showed that the change in the morphology and chemical structure of  $\text{Fe}_2\text{O}_3$ -KLN during the experiments was negligible. The amount of leached iron ( $\sim 0.006 \text{ mM}$ ) revealed that hydroxyl radicals were mainly produced by heterogeneous reactions of surface iron species. GC-MS, HPLC and LC-MS analysis allowed the identification of some of organic oxidation intermediates. Inorganic oxidation intermediates ( $\text{F}^-$ ,  $\text{NO}_3^-$  and  $\text{NH}_4^+$ ) were identified by IC analysis. An oxidation pathway was proposed for the mineralization of ENXN.

© 2016 Elsevier B.V. All rights reserved.

## 1. Introduction

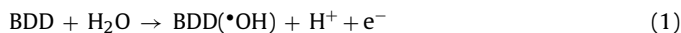
The treatment of persistent organic pollutants is a very important task these days to protect the environment and water resources. Of all the available treatment methods, advanced oxidation processes (AOPs) are the most promising methods because of their high oxidation ability, relatively low costs and easy applications. These processes generally use highly reactive intermediates (especially hydroxyl radical,  $\cdot\text{OH}$ ) to oxidize organic pollutants [1–8]. While there are many different methods such as chemical, sono-chemical and photo-chemical to produce hydroxyl radicals, electrochemical methods such as anodic oxidation and electro-Fenton are the most efficient and economic methods [1,2,5]. Anodic oxidation process uses a high over-potential anode such as boron doped diamond (BDD) to produce hydroxyl radicals (Eq. (1)), whereas electro-Fenton method is based on the propagation of Fenton's reaction (Eq. (2)) by means of electricity [1,2,9]. These reactions have to be performed throughout the treatment process because the produced hydroxyl radicals are very reactive and

unstable. While the first reaction (Eq. (1)) can be conducted by applying a suitable potential to anode surface [3,10], the second reaction (Eq. (2)) requires the continuous supply of  $\text{H}_2\text{O}_2$  and  $\text{Fe}^{2+}$  throughout the electrolysis. The required  $\text{H}_2\text{O}_2$  and  $\text{Fe}^{2+}$  can be obtained in reaction medium by reduction of  $\text{O}_2$  (Eq. (3)) and  $\text{Fe}^{3+}$  (Eq. (4)) at a suitable potential on a cathode surface, respectively [5,11–13]. The combination of anodic oxidation (Eq. (1)) and electro-Fenton method (Eq. (2)) prominently increases the oxidation ability of the system. In this hybrid system, electrolysis is conducted in an undivided electrochemical cell containing a BDD anode and a carbon based cathode [3,14,15]. A small quantity of  $\text{Fe}^{2+}$  or  $\text{Fe}^{3+}$  salt is added into the electrolysis solution. This hybrid process has been heavily investigated in the removal of persistent organic pollutants these days [1,2,5,6,13,16]. On the other hand, electro-Fenton method suffers from some common drawbacks of Fenton's reaction such as (i) the requirements of strict pH regulation between 2 and 4, (ii) the loss of soluble iron catalyst as hydroxide precipitate [17,18] and (iii) post-treatment requirements prior to discharge [18,19]. To overcome these drawbacks in classical Fenton treatments, many attempts have been performed on the use of heterogeneous catalyst containing iron oxides instead of soluble iron salts. In this frame, goethite was used as the heterogeneous iron source in the electro-Fenton treatment [20]. Pyrite has been

\* Corresponding author.

E-mail address: [aocan3@anadolu.edu.tr](mailto:aocan3@anadolu.edu.tr) (A. Özcan).

utilized as a heterogeneous iron source in the electro-Fenton treatment of tyrosol [21], levofloxacin [22] and an azo dye [23]. The use of Fe alginate gel beads in the electro-Fenton oxidation of imidacloprid was also reported [24]. Zubir et al. [25] have synthesized a graphene oxide-iron oxide nano-composite for the Fenton-like oxidation of acid orange 7. These studies showed that the performance of the heterogeneous electro-Fenton treatment was much higher than that of homogeneous treatment. As a result of this, the use of new composites containing iron species is worth to investigate for obtaining heterogeneous electro-Fenton treatment processes which have high oxidation ability towards organic pollutants. In this frame,  $\text{Fe}_2\text{O}_3$  modified kaolin ( $\text{Fe}_2\text{O}_3$ -KLN) can be seen a promising candidate as a heterogeneous catalyst for electro-Fenton process. Kaolin (KLN) is widely utilized as a catalyst support due to its low cost, good adsorption capacity and environmentally friendly structure [26]. The modification of KLN with  $\text{Fe}_2\text{O}_3$  has already been performed for the photo-Fenton degradation of rhodamine B [18]. Moreover, it was tested in the decolorization of wastewaters containing acid red-1 in a heterogeneous Fenton-like reaction [27]. On the other hand, little attention was paid to the use of  $\text{Fe}_2\text{O}_3$ -KLN in heterogeneous electro-Fenton process. There was only one study dealing with the use of  $\text{Fe}_2\text{O}_3$ -KLN in the electro-Fenton treatment of organic pollutants [28]. They have tested the catalytic activity of  $\text{Fe}_2\text{O}_3$ -KLN in the electro-catalytic oxidation of methylene blue using a pair of graphite electrode.



In this study, we investigated the preparation, characterization and application of  $\text{Fe}_2\text{O}_3$ -KLN as a heterogeneous catalyst for the electro-Fenton process in the presence of most-widely used electrodes; platinum, BDD and carbon felt. We selected enoxacin (ENXN), a fluoroquinolone antibiotic, as a model substance since the pollution problems especially antibiotic resistance arising from fluoroquinolone antibiotics have been increased lately [22,29–33]. The parameters affecting mineralization behaviour of ENXN during the heterogeneous electro-Fenton treatment were optimized. A systematic study was conducted on the identification of oxidation intermediates of ENXN in heterogeneous electro-Fenton treatment conditions after a careful evaluation of application conditions of  $\text{Fe}_2\text{O}_3$ -KLN. Gas chromatography-mass spectrometry (GC-MS), high-pressure liquid chromatography-mass spectrometry (LC-MS) and ion chromatography (IC) analysis indicated the formations of five different aromatic, eleven aliphatic and three inorganic intermediates during the electro-catalytic oxidation of ENXN. Taking into account these intermediates, an oxidation pathway was proposed for the heterogeneous electro-catalytic oxidation of ENXN. The results revealed that the use of  $\text{Fe}_2\text{O}_3$ -KLN as a heterogeneous catalyst brings many advantages such as higher mineralization efficiencies, lower loss of soluble iron species and application in a wide pH range.

## 2. Materials and methods

### 2.1. Materials

Enoxacin (99%) and kaolin were supplied from Sigma-Aldrich. Iron(III)sulphate pentahydrate (97%, Aldrich), sodium sulphate (anhydrous, 99%, Across), *p*-hydroxybenzoic acid (99.9%, Merck), sulfuric acid, (98%, Across), acetic acid (glacial p.a., Across), potassium hydrogen phthalate (Nacalai tesque Inc.) and N,O-bis(trimethylsilyl)trifluoroacetamide (Aldrich) were obtained as a

reagent grade. Sodium nitrate (99%, Merck), sodium fluoride (99%, Fluka), ammonium nitrate (99%), sodium carbonate (ACS reagent grade, Aldrich) and methanesulfonic acid (>99.0%, Fluka) were used in ion chromatography analysis. Oxalic (98%), maleic (99%), glyoxylic (98%), formic (98%) and oxamic (96%) acids were obtained from Fluka and used without further purification.

### 2.2. Procedures and equipment

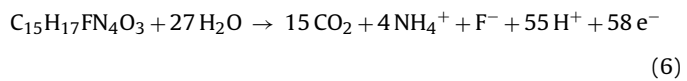
An undivided cylindrical glass cell, which has a diameter of 5.0 cm, was used in the experiments. A piece of three-dimensional carbon felt (70.0 cm<sup>2</sup>), placed on the inner wall of the cell covering the totality of the internal perimeter, was used as a cathode. A platinum gauze (Pt, 5 × 4 cm, 100 mesh, Sigma) or boron doped diamond (BDD, 5 × 4 cm, DIACHEM®) were used as anodes. Electrolysis solutions were prepared by dissolving a suitable amount of ENXN in distilled water containing 0.05 M Na<sub>2</sub>SO<sub>4</sub>. A catalytic quantity of  $\text{Fe}_2(\text{SO}_4)_3$  and  $\text{Fe}_2\text{O}_3$ -KLN was introduced into the solutions during the homogeneous and heterogeneous electro-Fenton experiments, respectively. The electrolysis medium was saturated with oxygen by bubbling compressed air and agitated continuously by a magnetic stirrer (500 rpm) throughout the electrolysis. The current values were measured by using a DC power supply (Hameg Triple Power Supply, HM8040-3).

After heterogeneous electro-Fenton experiments, the catalyst ( $\text{Fe}_2\text{O}_3$ -KLN) was recovered by filtration using an ordinary filter paper (Macherey-Nagel) and dried at 100 °C.

Mineralization current efficiency (MCE) of the electrolysis was calculated according to following equation (Eq. (5)) [4,23].

$$\text{MCE}(\%) = \frac{\Delta(\text{TOC})_t nFV_s}{4.32 \times 10^7 mIt} \times 100 \quad (5)$$

Here,  $\Delta(\text{TOC})_t$  shows the amount of TOC removal (mg carbon L<sup>-1</sup>) at a given time,  $m$  is the number of carbon atoms found in ENXN,  $F$  is Faraday constant (96487 C mol<sup>-1</sup>) and  $4.32 \times 10^7$  is the conversion factor for homogenization of units (=3600 s h<sup>-1</sup> × 12000 mg carbon mol<sup>-1</sup>),  $V_s$  is the volume of solution in liter (L),  $I$  is the applied current in ampere (A) and  $t$  is the electrolysis time in hour (h).  $n$  is the number of electrons exchanged per mole of ENXN, which is determined as 58 according to following equation (Eq. (6)).



### 2.3. Preparation and characterization of $\text{Fe}_2\text{O}_3$ -KLN

$\text{Fe}_2\text{O}_3$ -KLN catalyst was prepared by following the given steps. A suitable amount of kaolin (2.5 g) was dispersed in deionized water and stirred magnetically for 2 h. After that, 0.25 g  $\text{FeCl}_3 \cdot 6\text{H}_2\text{O}$  was added into the previous solution. After 4 h stirring, the pH of the mixture was adjusted to 7 by adding aqueous NaOH (0.5 M) solution. At this stage, the colour of the mixture was turned from straw coloured to brown. The formed brown precipitate was filtered and washed three times with distilled water and methanol. Finally, the precipitate was calcinated at 600 °C.

Characterization of the catalyst was performed by using scanning electron microscopy (SEM), X-ray diffraction (XRD), BET (Brunauer–Emmett–Teller) and atomic absorption spectrometry (AAS) analysis.

Surface morphologies of KLN,  $\text{Fe}_2\text{O}_3$ -KLN and used- $\text{Fe}_2\text{O}_3$ -KLN were investigated by an Ultra High Resolution Field Emission Scanning Electron Microscope (ULTRAFE-SEM, Zeiss-Ultraplus). Elemental compositions of KLN,  $\text{Fe}_2\text{O}_3$ -KLN and  $\text{Fe}_2\text{O}_3$ -KLN were determined by an ULTRAFE-SEM equipped with an energy disper-

sive X-ray (EDX) detector using an accelerating voltage of 15 kV and a magnification of 1000 $\times$ .

XRD measurements were conducted by a BRUKER D8 Advance X-ray diffractometer. Data were collected in the angular region of  $2\theta = 10\text{--}90^\circ$  in a step-scanning mode, with a step length of  $0.01^\circ$ .

Surface areas of KLN, Fe<sub>2</sub>O<sub>3</sub>-KLN and used-Fe<sub>2</sub>O<sub>3</sub>-KLN were determined by BET method using a surface analyzer (Quantachrome Inst., Nova 2200e).

Iron loads of Fe<sub>2</sub>O<sub>3</sub>-KLN and used-Fe<sub>2</sub>O<sub>3</sub>-KLN were determined by mixing Fe<sub>2</sub>O<sub>3</sub>-KLN (0.025 g) or used-Fe<sub>2</sub>O<sub>3</sub>-KLN (0.025 g) with conc. HCl (50 mL) and subsequent determination of dissolved iron by a flame atomic absorption spectrometer (PerkinElmer AAnalyst 800).

#### 2.4. Analytical methods

ENXN concentrations during the electrolysis were monitored by high performance liquid chromatography (HPLC). Mineralization behaviours of ENXN and its intermediates were followed by total organic carbon (TOC) analysis. Released carboxylic acids and inorganics ions were determined by ion-exclusion chromatography and ion-exchange chromatography analysis, respectively. Gas chromatography-mass spectrometry (GC-MS) and liquid chromatography-mass spectrometry (LC-MS) analysis was used for the identification of aromatic oxidation intermediates of ENXN. Details of analytical systems that used in this study were given in the Supporting information File.

#### 2.5. Identification of radical species

Radical scavenging studies were performed to evaluate the formed dominant radicals during the heterogeneous electro-Fenton treatment of ENXN with Fe<sub>2</sub>O<sub>3</sub>-KLN catalyst. For this purpose, heterogeneous electro-Fenton treatment of 0.25 mM ENXN was conducted at 60 mA in the absence and presence of radical scavengers. Benzoquinone (BQ, 0.02 mM) and *tert*-butyl alcohol (TBA, 5% v/v) were used as scavengers for superoxide radical ( $\bullet\text{O}_2^-$ ) and hydroxyl radical ( $\bullet\text{OH}$ ), respectively [34].

### 3. Results and discussion

#### 3.1. Characterization of Fe<sub>2</sub>O<sub>3</sub>-KLN

The prepared heterogeneous catalyst (Fe<sub>2</sub>O<sub>3</sub>-KLN) was characterised by using different methods. Firstly, SEM images of KLN, Fe<sub>2</sub>O<sub>3</sub>-KLN and used-Fe<sub>2</sub>O<sub>3</sub>-KLN were obtained (Fig. 1). KLN is composed of particles having different irregular shapes and sizes (Fig. 1A). As can be seen, there was no significant change in the morphology of KLN after modification with Fe<sub>2</sub>O<sub>3</sub> (Fig. 1B). This indicated that there was a rather uniform distribution throughout the KLN surface rather than an unusual deposition of Fe<sub>2</sub>O<sub>3</sub>. SEM image of used-Fe<sub>2</sub>O<sub>3</sub>-KLN is very similar to that of Fe<sub>2</sub>O<sub>3</sub>-KLN (Fig. 1C) indicating no change occurred in the morphology of Fe<sub>2</sub>O<sub>3</sub>-KLN during the electro-Fenton experiments. EDX analysis of Fe<sub>2</sub>O<sub>3</sub>-KLN and used-Fe<sub>2</sub>O<sub>3</sub>-KLN verified the presence of iron in the prepared catalyst structures.

XRD diffraction patterns of KLN, Fe<sub>2</sub>O<sub>3</sub>-KLN and used-Fe<sub>2</sub>O<sub>3</sub>-KLN were obtained to evaluate the modification of KLN with Fe<sub>2</sub>O<sub>3</sub> (Fig. 2). The observed diffraction peaks ( $2\theta$ : 12.43°, 20.39°, 20.76°, 21.26°, 24.95°, 26.69°, 34.98°, 35.40°, 35.96°, 36.38°, 37.70°, 38.42°, 39.24°, 39.96°, 45.36°, 54.98° and 62.23°) showed the high crystallinity of KLN (Fig. 2A) [18,35]. On the contrary to KLN, the prepared Fe<sub>2</sub>O<sub>3</sub>-KLN and used-Fe<sub>2</sub>O<sub>3</sub>-KLN showed more amorphous structures (Fig. 2B and C). The dominant peaks observed in XRD patterns of Fe<sub>2</sub>O<sub>3</sub>-KLN and used-Fe<sub>2</sub>O<sub>3</sub>-KLN were also attributed to KLN structure (Fig. 2B and C). On the other hand, the intensities of

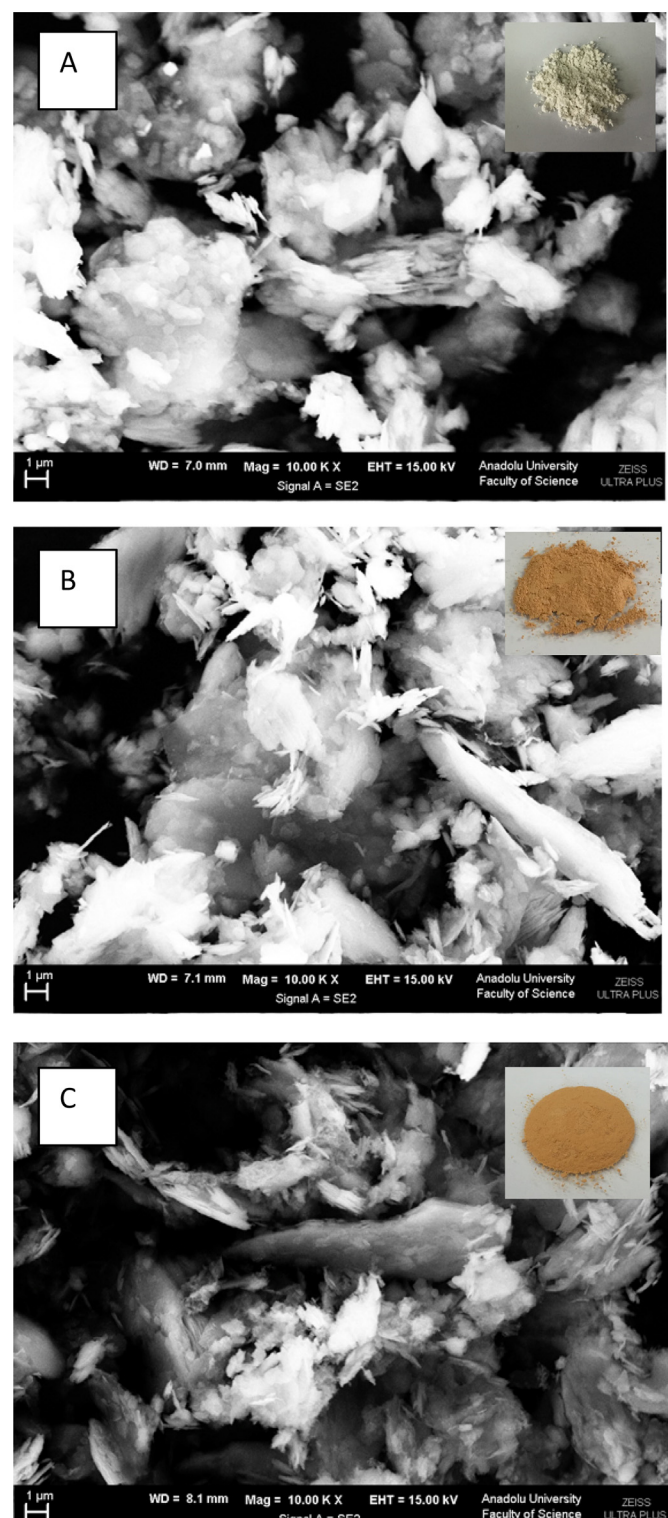


**Fig. 1.** SEM images of KLN (A), Fe<sub>2</sub>O<sub>3</sub>-KLN (B) and used-Fe<sub>2</sub>O<sub>3</sub>-KLN (C). Insets show the optical images.

these peaks prominently decreased after the modification process. This may arise from the calcination process that applied during the preparation of Fe<sub>2</sub>O<sub>3</sub>-KLN. Similar findings were also reported in the literature [18]. The diffraction peaks observed at  $2\theta$  values of 33.15° (a), 35.61° (b), 40.86° (c), 49.48° (d), 54.09° (e), 57.59° (f), 62.45° (g) and 63.99° (h) were ascribed to Fe<sub>2</sub>O<sub>3</sub> (JCPDS No. 33-0664) (Fig. 2-inset). These peaks verified the presence of

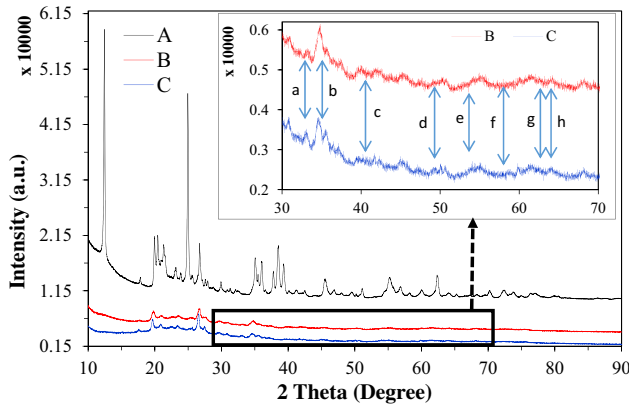


**Fig. 2.** XRD patterns of KLN (A), Fe<sub>2</sub>O<sub>3</sub>-KLN (B) and used-Fe<sub>2</sub>O<sub>3</sub>-KLN (C).

Fe<sub>2</sub>O<sub>3</sub> (hematite) in both Fe<sub>2</sub>O<sub>3</sub>-KLN and used-Fe<sub>2</sub>O<sub>3</sub>-KLN structures. The intensities of the observed peaks are very low according to peaks that come from KLN. This arises from the low amount of iron (2.0–1.9% obtained from AAS analysis) in Fe<sub>2</sub>O<sub>3</sub>-KLN and used-Fe<sub>2</sub>O<sub>3</sub>-KLN structures. It is important to note that the XRD patterns of Fe<sub>2</sub>O<sub>3</sub>-KLN and used-Fe<sub>2</sub>O<sub>3</sub>-KLN are almost same (Fig. 2B and Fig. 2C). This indicates that the structure of Fe<sub>2</sub>O<sub>3</sub>-KLN does not significantly change during the heterogeneous electro-Fenton treatments.

The amounts of iron loads of Fe<sub>2</sub>O<sub>3</sub>-KLN and used-Fe<sub>2</sub>O<sub>3</sub>-KLN were determined by AAS analysis. The Fe<sub>2</sub>O<sub>3</sub>, found on the catalyst surface, was dissolved with concentrated HCl and AAS analysis of the formed solution was performed. The loaded amounts of iron were calculated as 20.06 ( $\pm 0.19$ ) mg Fe/g KLN and 18.96 ( $\pm 0.25$ ) mg Fe/g KLN for Fe<sub>2</sub>O<sub>3</sub>-KLN and used-Fe<sub>2</sub>O<sub>3</sub>-KLN, respectively. The determined amount of iron on Fe<sub>2</sub>O<sub>3</sub>-KLN is very close to the used amount of iron (20.55 mg Fe/g KLN) during the catalyst preparation procedure.

The surface areas of KLN, Fe<sub>2</sub>O<sub>3</sub>-KLN and used-Fe<sub>2</sub>O<sub>3</sub>-KLN were determined by BET analysis as 34.98 ( $\pm 0.23$ ), 40.58 ( $\pm 0.26$ ) and 39.32 ( $\pm 0.31$ ) m<sup>2</sup> g<sup>-1</sup>, respectively. As can be seen, the surface area of KLN increased in the presence of Fe<sub>2</sub>O<sub>3</sub>. A slight difference was observed in the surface areas of Fe<sub>2</sub>O<sub>3</sub>-KLN and used-Fe<sub>2</sub>O<sub>3</sub>-KLN. This revealed that electro-Fenton experiments did not lead to any noticeable alteration in the morphology and chemical structure of Fe<sub>2</sub>O<sub>3</sub>-KLN.

### 3.2. Comparative degradation behaviour of ENXN in homogeneous and heterogeneous electro-Fenton treatment

Mineralization behaviour of ENXN was investigated by homogeneous and heterogeneous electro-Fenton methods at 60 mA to evaluate the catalytic activity of Fe<sub>2</sub>O<sub>3</sub>-KLN (Fig. 3). The catalyst concentrations used in homogeneous and heterogeneous electro-Fenton experiments were 0.3 mM Fe<sup>3+</sup> and 0.1 g Fe<sub>2</sub>O<sub>3</sub>-KLN, respectively. At these conditions, mineralization rates of ENXN were very close to each other in homogeneous and heterogeneous systems when the experiments performed with Pt/CF electrode combination (Fig. 3b and c). On the other hand, a noticeable increase was observed in the mineralization rates of ENXN in both systems when Pt replaced with BDD (Fig. 3d and e). The mineralization rate of ENXN reached to its maximal value in heterogeneous electro-Fenton treatment with Fe<sub>2</sub>O<sub>3</sub>-KLN at the studied conditions. These results indicate that the prepared catalyst shows high catalytic activity in the electro-Fenton removal of ENXN. Similar results were observed for the heterogeneous electro-Fenton treatments of tyrosol [21], levofloxacin [22] and an azo dye [23] using pyrite as a catalyst. It is important to note that degradation rates of ENXN in

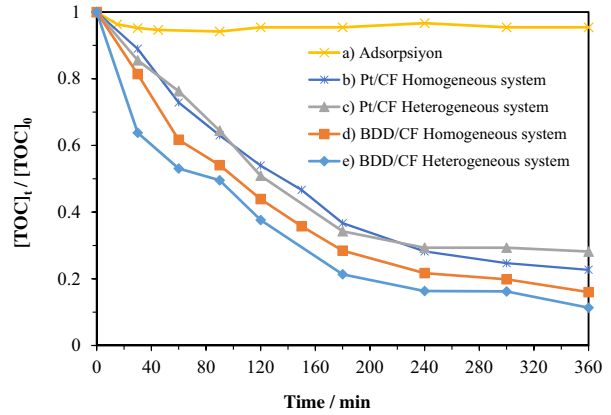


**Fig. 3.** Relative TOC removal values of ENXN during the adsorption on Fe<sub>2</sub>O<sub>3</sub>-KLN (a) and different electro-Fenton treatment processes in homogeneous and heterogeneous systems by Pt/CF (b and c) and BDD/CF (d and e) electrode combinations. C<sub>ENXN</sub>: 0.25 mM, [Na<sub>2</sub>SO<sub>4</sub>]: 0.05 M, [Fe<sup>3+</sup>]: 0.3 mM (b and d), m(Fe<sub>2</sub>O<sub>3</sub>-KLN): 0.1 g (c and e), I: 60 mA, pH: 3.0, V: 0.175 L, T: 25 °C.

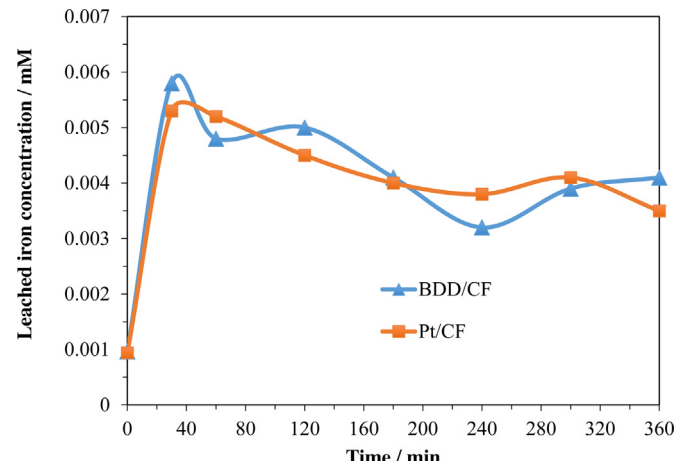


**Fig. 4.** Leached iron concentrations during the heterogeneous electro-Fenton treatment of ENXN in the presence of 0.3 g Fe<sub>2</sub>O<sub>3</sub>-KLN using electrode combinations of BDD/CF and Pt/CF. C<sub>ENXN</sub>: 0.25 mM, [Na<sub>2</sub>SO<sub>4</sub>]: 0.05 M, m(Fe<sub>2</sub>O<sub>3</sub>-KLN): 0.3 g, I: 60 mA, pH: 5.1, V: 0.175 L, T: 25 °C.

both systems can show different characteristics depending on the used amount of the catalysts. To determine the effect of the adsorption process on the mineralization rate, Fe<sub>2</sub>O<sub>3</sub>-KLN was added into ENXN solution and TOC of the solution was measured at different time periods (Fig. 3a). TOC values of the solution were almost the same indicating there was no adsorption of ENXN on Fe<sub>2</sub>O<sub>3</sub>-KLN. In homogeneous electro-Fenton treatment, mineralization of ENXN arises from the reaction of ENXN with hydroxyl radicals which are produced both in electrolysis medium (Eq. (2)) and anode surface (Eq. (1)). A third source for the production of hydroxyl radical is also available in the case of heterogeneous electro-Fenton treatments from the reaction of hydrogen peroxide with surface iron species of the catalyst (Eq. (7)) [19,25]. As a result of this, the mineralization rate of ENXN was much faster in heterogeneous system than that of homogeneous one. To evaluate the importance of the heterogeneous reaction in the production of hydroxyl radicals, iron concentrations leached from the added Fe<sub>2</sub>O<sub>3</sub>-KLN were quantified by atomic absorption spectrometry analysis. The obtained results are presented in Fig. 4. A very small amount ( $\sim 0.001$  mM = 0.056 ppm) of dissolved iron found in solution at the beginning of the electrolysis. The leached iron concentration reached to its highest value ( $\sim 0.006$  mM = 0.336 ppm) at the first 30 min. After that time, the iron concentrations decreased slowly

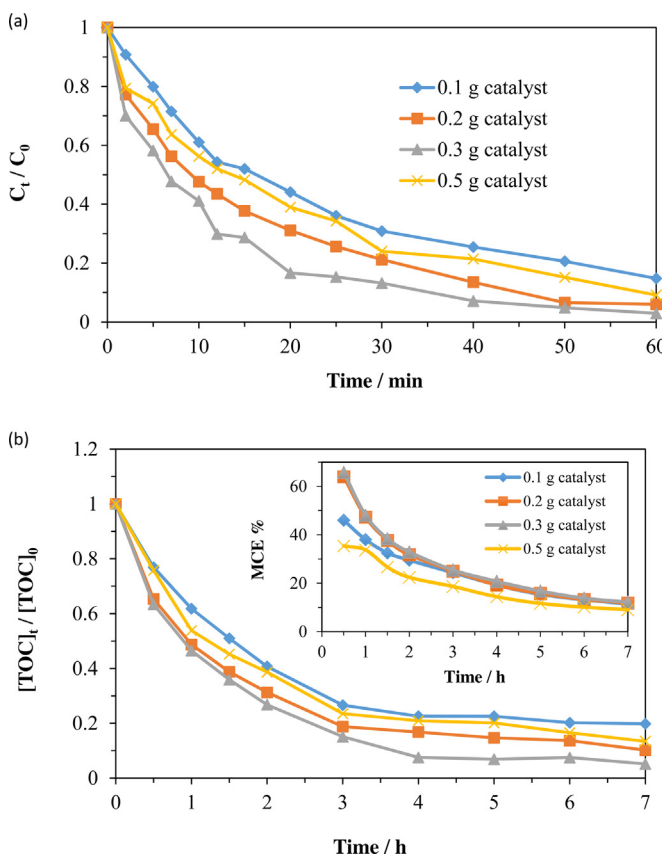
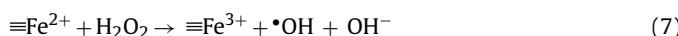


**Fig. 5.** The effect of the amount of catalyst ( $\text{Fe}_2\text{O}_3$ -KLN) on the degradation (a) and mineralization (b) rates of ENXN during the electro-Fenton treatment by BDD/CF.  $C_{\text{ENXN}}$ : 0.25 mM,  $[\text{Na}_2\text{SO}_4]$ : 0.05 M, I: 60 mA, pH: 5.1, V: 0.175 L, T: 25 °C. Inset shows the MCE values.

and reached a plateau ( $\sim 0.004 \text{ mM} = 0.224 \text{ ppm}$ ). Similar results were noted during the photo-Fenton degradation of rhodamine B using  $\text{Fe}_2\text{O}_3$ -KLN catalyst [18]. It is important to note that leached iron concentrations are very small according to the added amount of iron ( $0.3 \text{ mM} = 16.8 \text{ ppm}$ ) in homogeneous systems. From here, it can be concluded that hydroxyl radicals are mainly produced in the electrolysis medium from the heterogeneous reaction (Eq. (7)) instead of homogeneous reaction (Eq. (2)).



### 3.3. Optimization of parameters for heterogeneous electro-Fenton treatment of ENXN

The parameters influencing the performance of the system such as catalyst amount, applied current, initial pH, types of supporting electrolyte, temperature and initial ENXN concentration were optimized to increase the performance of the heterogeneous electro-Fenton treatment system.

#### 3.3.1. Optimization of catalyst amount

The effects of  $\text{Fe}_2\text{O}_3$ -KLN amount on the degradation and mineralization rates of ENXN were examined by performing electrolysis in the presence of increasing amounts of  $\text{Fe}_2\text{O}_3$ -KLN (Fig. 5). Degradation (Fig. 5a) and mineralization (Fig. 5b) of ENXN were followed by high performance liquid chromatography (HPLC) and total organic carbon (TOC) analysis, respectively. After 10 min electrolysis with 0.3 g  $\text{Fe}_2\text{O}_3$ -KLN, the concentration of ENXN decreased to 58% of its initial value (Fig. 5a). In the presence of 0.1 g, 0.2 g and 0.5 g  $\text{Fe}_2\text{O}_3$ -KLN, ENXN concentrations decreased to 39%, 52% and 43% of the initial values, respectively. The complete degradation

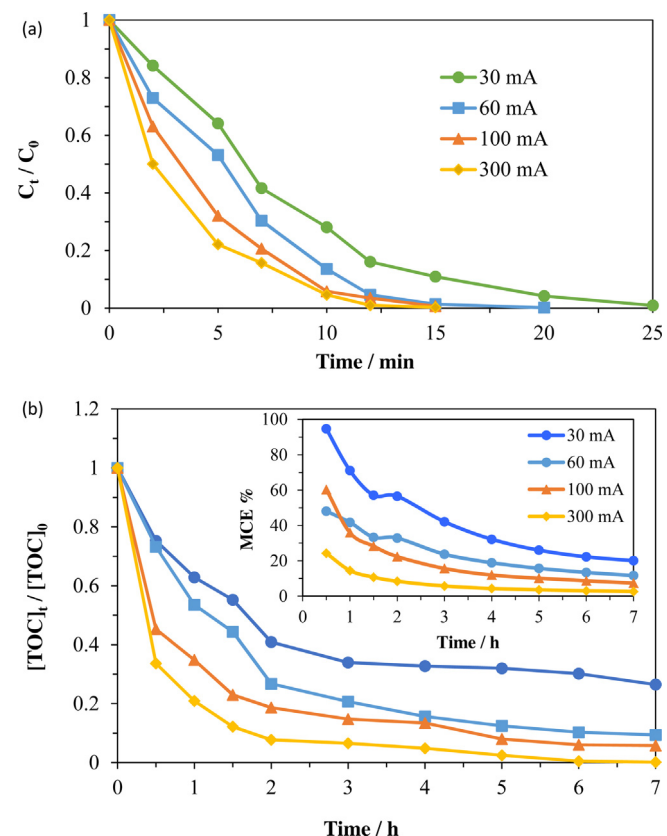


**Fig. 6.** The effect of applied current on the degradation (a) and mineralization (b) rates of ENXN during the heterogeneous electro-Fenton treatment.  $C_{\text{ENXN}}$ : 0.25 mM,  $m(\text{Fe}_2\text{O}_3\text{-KLN})$ : 0.3 g, V: 0.175 L, T: 25 °C,  $[\text{Na}_2\text{SO}_4]$ : 0.05 M. Inset shows the MCE values.

of ENXN took almost 60 min in the presence of 0.3 g  $\text{Fe}_2\text{O}_3$ -KLN. In the case of other amounts of  $\text{Fe}_2\text{O}_3$ -KLN, complete degradation required much higher time values. A very similar trend was seen in mineralization rates (Fig. 5b). The different degradation and mineralization rates of ENXN in the presence of different amounts of  $\text{Fe}_2\text{O}_3$ -KLN can be explained by taking into account the heterogeneous and homogeneous reactions. The increase in the amount of  $\text{Fe}_2\text{O}_3$ -KLN increases both the catalytic iron surfaces and dissolved amount of iron species. While the increase of these species increases the number of hydroxyl radicals, parasitic reactions (Eqs. (8) and (9)) that consume hydroxyl radicals may also increase in the electrolysis medium [6,15,36]. The observed slight decrease in the degradation and mineralization rates of ENXN arises from the presence of these reactions (Eqs. (8) and (9)). MCE values showed that the efficiencies of the electrolysis reached to their maximal values (35.34–65.71%) after thirty minutes treatment (Fig. 5b-inset). After that time, a gradual decrease was seen in MCE values.



#### 3.3.2. Optimization of applied current

The effect of applied current on the degradation and mineralization rates of ENXN has been examined by performing electrolysis at different applied current values (Fig. 6). There was an increase in the degradation rates of ENXN by the increase of the applied current from 30 to 300 mA. This increase was very prominent at first 5 min. The complete degradation of ENXN required 25, 20, 17 and 15 min for the applied current values of 30, 60, 100 and 300 mA, respectively (Fig. 6a). Similar results have been previously observed during homogeneous electro-Fenton treatments [6,13,16]. Miner-

alization rates of ENXN were also affected by the applied current change (Fig. 6b). After 7 h treatments with  $\text{Fe}_2\text{O}_3$ -KLN, 98% of the initial TOC ( $36.33 \text{ mg L}^{-1}$ ) were removed from the electrolysis medium at 300 mA. TOC removal values of 71%, 88% and 92% were observed at applied current values of 30, 60 and 100 mA, respectively. These results indicate that total mineralization of ENXN can be achieved for all current values at these conditions but the required time depends on the amount of applied current. This situation arises from the higher production rate of hydrogen peroxide on the cathode surface and hydroxyl radicals on the anode surface at higher current values. As can be seen, there is no linear relationship between the observed TOC removal and applied current. This may arise from the presence of parasitic electrochemical reactions such as the oxidation of water to form  $\text{O}_2$  instead of hydroxyl radical on BDD (Eq. (10)) and the reduction of  $\text{O}_2$  to form  $\text{H}_2\text{O}$  instead of  $\text{H}_2\text{O}_2$  on CF (Eq. (11)). These parasitic reactions determine the upper limit of the applied current value. While the mineralization rate of ENXN was not very high at 30 mA, the highest MCE values were observed at this current value (Fig. 6b-inset). MCE values prominently decreased by the increase of applied current from 30 to 300 mA. This indicates that the increase of applied current prominently increases the amount of parasitic reactions.



### 3.3.3. The effect of initial pH of the electrolysis solution

Homogeneous electro-Fenton experiments are generally performed at lower pH values than 4 because of the precipitation of the catalyst as ferric hydroxides at higher pH values [2,5]. This requires pH adjustment before and after electrolysis. Heterogeneous catalysts may overcome this drawback of homogeneous systems. The effect of initial pH on the degradation and mineralization rates of ENXN solutions during the heterogeneous electro-Fenton treatment with  $\text{Fe}_2\text{O}_3$ -KLN was examined (Fig. 7). The electrolysis was conducted by changing the initial pH of the ENXN solutions. Firstly, experiments were performed without any pH adjustment at 5.1, which is the native pH of ENXN solution. At this pH value, the complete removal of ENXN took 60 min, but it completed in 20 min at pH values of 2.0 and 3.0 (Fig. 7a). The decrease of the initial pH value from the native value of 5.1 to smaller values led to a sharp increase in the degradation rates of ENXN (Fig. 7a). On the other hand, the increase of initial pH value up to 7.1 led to a prominent decrease in the degradation rates of ENXN. Similar trends were found in the mineralization experiments of ENXN at different pH values (Fig. 7b). This situation may result from the different efficiencies of the Fenton's reaction at different pH values. The efficiency of the Fenton's reaction was the best at pH range of 2.0 and 4.0 [1,5,11]. Therefore, higher degradation and mineralization rates of ENXN were observed at pH values of 2.0 and 3.0. While the degradation and mineralization rates of ENXN were much faster at low pH values, the complete degradation and mineralization of ENXN were reached at all studied pH values. The pH of the electrolysis medium was followed with a pH meter but not regulated during the experiments. It was observed that the pH values of electrolysis mediums decreased to 1.98, 2.87, 3.87 and 4.35 from the initial values of 2, 3, 5.1 and 7.1 after 7 h treatment. The observed pH decreases arise from the formation of short-chain carboxylic acids during the mineralization of ENXN. These pH drops explain the higher mineralization rates of ENXN for the systems that have initial pH values of 5.1 and 7.1 at the final stage of the electrolysis. These results reveal that the proposed heterogeneous electro-Fenton method can be used in a wide pH range without any pH adjustment. In parallel to mineralization rates, MCE values also decreased by the increase of initial pH values at the initial stage of the electrolysis (Fig. 7b-inset).

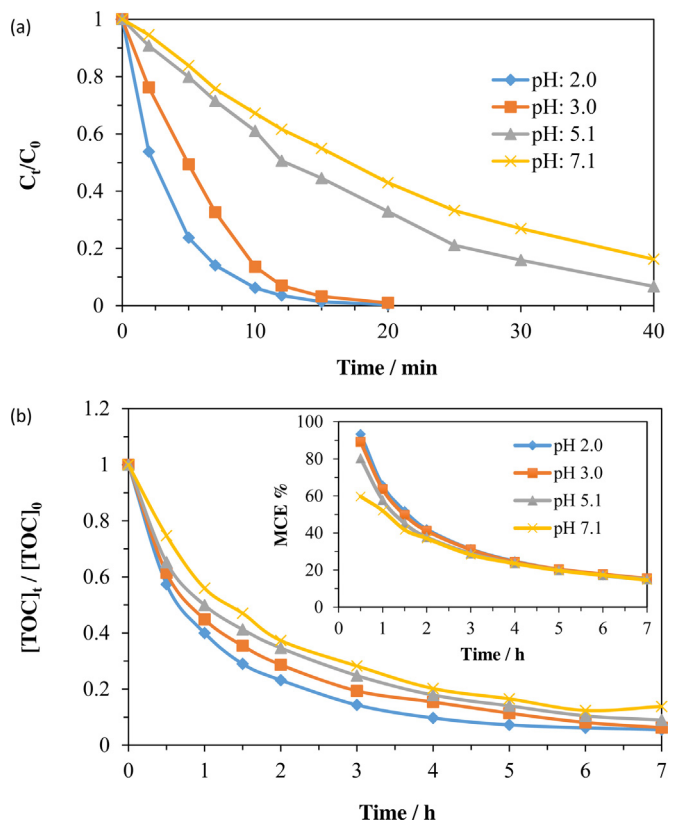
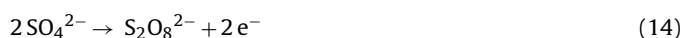
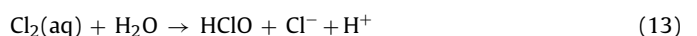


**Fig. 7.** The effect of pH on the degradation (a) and mineralization (b) rates of ENXN during the heterogeneous electro-Fenton treatment.  $C_{\text{ENXN}}: 0.25 \text{ mM}$ ,  $[\text{Na}_2\text{SO}_4]: 0.05 \text{ M}$ ,  $m(\text{Fe}_2\text{O}_3\text{-KLN}): 0.3 \text{ g}$ ,  $I: 60 \text{ mA}$ ,  $V: 0.175 \text{ L}$ ,  $T: 25^\circ\text{C}$ . Inset shows the MCE values.

After 2 h electrolysis, MCE values were almost same for all studied pH values.

### 3.3.4. Optimization of types of supporting electrolyte

The effects of three commonly used sodium salts ( $\text{NaCl}$ ,  $\text{NaNO}_3$  and  $\text{Na}_2\text{SO}_4$ ) on the degradation and mineralization rates of ENXN were evaluated (Fig. 8). Degradation rates of ENXN were almost the same in the presence of  $\text{NaCl}$  and  $\text{Na}_2\text{SO}_4$ , but it prominently decreased in the presence of  $\text{NaNO}_3$  (Fig. 8a). Mineralization rates of ENXN (Fig. 8b) and obtained MCE values (Fig. 8b-inset) were much lower in the presence of  $\text{NaCl}$  and  $\text{NaNO}_3$  than that of  $\text{Na}_2\text{SO}_4$ . While the degradation rates of ENXN were much close to each other in the presence of  $\text{NaCl}$  and  $\text{Na}_2\text{SO}_4$ , there was a prominent difference between the mineralization rates of ENXN. These differences can be attributed to the inhibiting and promoting reactions of supporting electrolytes. It was reported that chloride was oxidized on the anode surface to form chlorine (Eq. (12)) and the liberated chlorine led to the formation of hypochlorous acid (Eq. (13)) [32]. While these species react with ENXN and its intermediates, their oxidation power is smaller than hydroxyl radical. These lead to slower mineralization rates of ENXN. The sulphate was also oxidized to form peroxydisulfate ions (Eq. (14)) [22]. The oxidation power of these ions is much higher than that of chlorine and hypochlorous acid. This explains the higher mineralization rate of ENXN in sulphate medium.



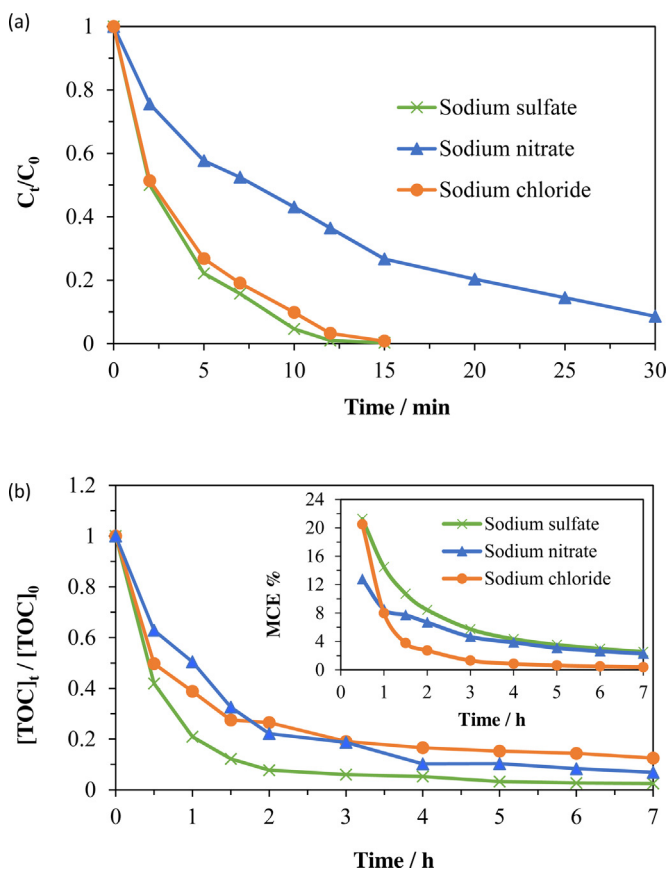


**Fig. 8.** The effect of supporting electrolyte on the degradation (a) and mineralization (b) rates of ENNX during the heterogeneous electro-Fenton treatment.  $C_{ENNX}$ : 0.25 mM, m( $\text{Fe}_2\text{O}_3$ -KLN): 0.3 g, pH: 3.0, I: 300 mA, V: 0.175 L, T: 25 °C. Inset shows the MCE% values.

### 3.3.5. The effect of temperature and initial concentration of ENNX

The effect of temperature was tested by performing electrolysis at 15 °C, 25 °C and 35 °C (Fig. 9). The degradation and mineralization rates of ENNX increased by the increase of temperature values from 15 °C to 35 °C. While the complete disappearance of ENNX took 25 min at 15 °C, it took only 10 min at 35 °C (Fig. 9a). The effect of temperature on the mineralization rate of ENNX was not so prominent (Fig. 9b). As can be seen, a small difference was observed in the MCE values in the first hour (Fig. 9b-inset). After that time, MCE values were almost same for all temperature values in parallel to the TOC removal values. The increase of temperature increases the energies of the reactants and the reaction rates. It also increases the mass transfer rates of species, which increases the rates of surface and bulk reactions [37]. On the other hand, the increase in temperature leads to a decrease in the amount of dissolved  $\text{O}_2$  and an increase in the decomposition rate of  $\text{H}_2\text{O}_2$  [37]. The total effects of these factors govern the degradation and mineralization rates of ENNX.

Finally, the effect of initial concentration of ENNX was examined by conducting the experiments using 0.125 mM, 0.25 mM and 0.5 mM ENNX (Fig. 10). A gradual decrease was observed in the degradation rates of ENNX by increasing the initial concentration of ENNX from 0.125 mM to 0.50 mM (Fig. 10a). On the contrary to degradation rates, a gradual increase was seen in the mineralization rates of ENNX (Fig. 10b). These behaviours can be explained by the constant production rate of  $\cdot\text{OH}$  at the studied conditions [38]. The reaction of ENNX with  $\cdot\text{OH}$  leads to the formation of by-products, which also react with  $\cdot\text{OH}$  because of its low selectivity. When the initial concentration of ENNX increased, the concentrations of

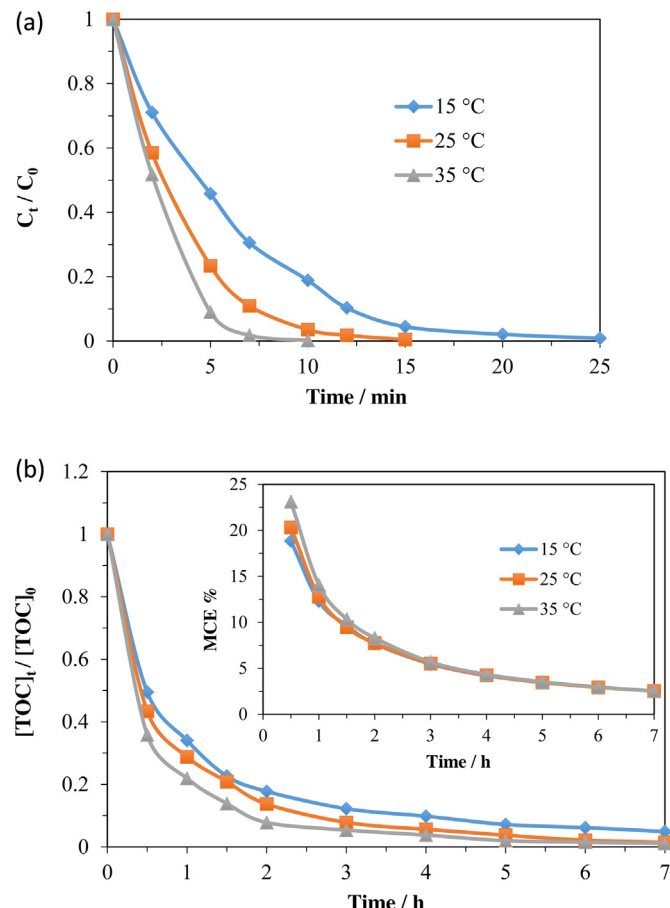


**Fig. 9.** The effect of temperature on the degradation (a) and mineralization (b) rates of ENNX during the heterogeneous electro-Fenton treatment.  $C_{ENNX}$ : 0.25 mM, m( $\text{Fe}_2\text{O}_3$ -KLN): 0.3 g, pH: 3.0, I: 300 mA, V: 0.175 L,  $[\text{Na}_2\text{SO}_4]$ : 0.05 M, Inset shows the MCE values.

by-products also increased. This situation decreases the effective concentration of  $\cdot\text{OH}$  and reaction rates. This is the main reason for the observed lower reaction rates at higher initial concentration of ENNX. On the other hand, TOC removal values and mineralization rates increased at higher ENNX concentrations because of the presence of higher concentration of organics in the electrolysis medium. The obtained results were compatible with the literature [39]. MCE values were also increased by the increase of the initial concentrations of ENNX from 0.125 mM to 0.5 mM (Fig. 10b-inset).

### 3.3.6. Reusability of $\text{Fe}_2\text{O}_3$ -KLN

Reusability of catalyst is another critical parameter for the heterogeneous catalytic systems. Reusability of  $\text{Fe}_2\text{O}_3$ -KLN was tested by repeating the electrolysis five-times using the same catalyst. After each trial, TOC values of the system have been determined. After 7 h electrolysis at 300 mA, TOC removal values of 98.1%, 97.9%, 98.0%, 97.6% and 97.7% were obtained in the successive experiments. A very insignificant loss (0.5%) was observed in the catalytic activity of  $\text{Fe}_2\text{O}_3$ -KLN catalyst. These results indicate that  $\text{Fe}_2\text{O}_3$ -KLN is a very suitable candidate for the heterogeneous electro-Fenton treatment of ENNX.

### 3.4. Determination of oxidation rate constant of ENNX

Theoretical aspects of reaction kinetic of the oxidation of organic substances with hydroxyl radicals in electrochemical advanced oxidation processes are well established in the literature [1,4,5,9,11,39,40]. The main oxidant in these systems is the

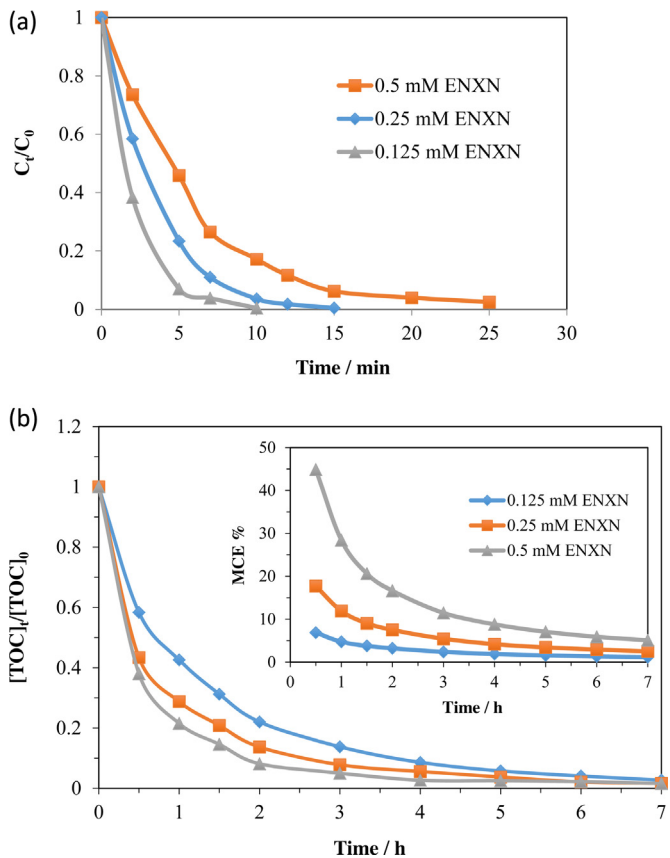


**Fig. 10.** The effect of initial concentration of ENNXN on the degradation (a) and mineralization (b) rates during the heterogeneous electro-Fenton treatment.  $C_{ENNXN}$ : 0.25 mM, m( $\text{Fe}_2\text{O}_3$ -KLN): 0.3 g, pH: 3.0, I: 300 mA, V: 0.175 L,  $[\text{Na}_2\text{SO}_4]$ : 0.05 M, Inset shows the MCE values.

hydroxyl radical and the reaction between organic substances and hydroxyl radical follows a second-order reaction kinetic [1,2,5]. The second-order oxidation rate constant of organic substances can be experimentally determined by competition kinetic experiments [11,39,41]. We have used these experiments to determine the second-order oxidation rate constant of ENNXN. In these experiments, *p*-hydroxybenzoic acid was served as a standard competitor whose rate constant reported as  $2.1 \times 10^9 \text{ M}^{-1} \text{ s}^{-1}$  [42]. Heterogeneous electro-Fenton experiments were performed at 25 °C and 60 mA using an electrolysis solution containing 0.25 mM ENNXN, 0.25 mM *p*-hydroxybenzoic acid, 0.3 g  $\text{Fe}_2\text{O}_3$ -KLN and 0.05 M  $\text{Na}_2\text{SO}_4$ . The second-order oxidation rate constant of ENNXN was calculated as  $1.24 (\pm 0.04) \times 10^9 \text{ M}^{-1} \text{ s}^{-1}$  using the equations given in the literatures [5,7,15]. This value lies in the acceptable range of second-order oxidation rate constants for the reactions of aromatic compounds with hydroxyl radicals [2,43,44]. There was no report for the comparison, which was related with the determination of second order-oxidation rate constant of ENNXN.

### 3.5. Determination of oxidation intermediates of ENNXN

A systematic study including successive three steps was conducted to determine the oxidation intermediates of ENNXN formed during the heterogeneous electro-Fenton treatment with  $\text{Fe}_2\text{O}_3$ -KLN catalyst. These steps include identification of aromatic intermediates, short-chain carboxylic acids and inorganic ions.

In the first step, Studies were focused on the identification of aromatic oxidation intermediates. Heterogeneous electro-Fenton treatment of ENNXN with  $\text{Fe}_2\text{O}_3$ -KLN catalyst was performed to prepare analysis samples. Liquid-liquid extractions of samples were

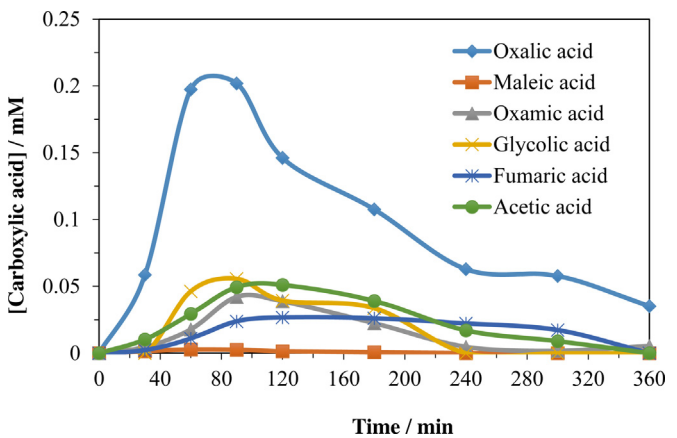


**Fig. 11.** The concentration-time profiles of generated short-chain carboxylic acids during the heterogeneous electro-Fenton treatment of ENNXN.  $C_{ENNXN}$ : 0.25 mM,  $[\text{Na}_2\text{SO}_4]$ : 0.01 M, m( $\text{Fe}_2\text{O}_3$ -KLN): 0.3 g, I: 60 mA, pH: 5.1, V: 0.175 L, T: 25 °C.

performed with dichloromethane and ethyl acetate. The obtained extracts were analysed by a gas chromatography-mass spectrometry (GC-MS) system. We have not obtained any meaningful results due to the polar structures of ENNXN and its oxidation intermediates. Therefore, a derivatization procedure was employed in GC-MS analysis using  $N,O$ -(bistrimethylsilyl)trifluoroacetamide to increase the volatilities of oxidation intermediates of ENNXN. All the identified intermediates showed aliphatic character (Table SM-1). Therefore, liquid chromatography-mass spectrometry (LC-MS) analysis was also conducted to determine aromatic intermediates. We identified five different aromatic oxidation intermediates (Table SM-2). Annabi et al. [45] reported the formation of aromatic oxidation intermediates during the homogeneous electro-Fenton treatment of ENNXN. They reported that the formations of ten aromatic intermediates, but all of the reported intermediates differ from that of ours. The formation of our oxidation intermediates is more reasonable according to the literature studies [22,32].

In the second step, identification and quantification of generated short-chain carboxylic acids were conducted. Electrolysis solutions were analysed by a high performance liquid chromatography (HPLC) system including an ion-exclusion column. The formation of six different short-chain carboxylic acids was observed during the heterogeneous electro-Fenton treatment of ENNXN with  $\text{Fe}_2\text{O}_3$ -KLN catalyst. These substances can be listed as below; oxalic acid, oxamic acid, maleic acid, fumaric acid, acetic acid and glycolic acid. Annabi et al. [45] reported the formation of acetic and oxalic acids during the homogeneous electro-Fenton treatment of ENNXN but they did not observe the formation of oxamic, maleic, fumaric and glycolic acids. The concentration-time profiles of the identified carboxylic acids are shown in Fig. 11. The concentrations of all carboxylic acids were very small in the first 30 min. A tremendous increase was noted in the concentration of carboxylic acids especially in oxalic acid up to 60 min. After 90 min, concentrations of carboxylic acids gradually decreased to very small values. The same analysis was also repeated with samples prepared by homogeneous electro-Fenton treatment of ENNXN to evaluate the differences between homogenous and heterogeneous systems. A similar tendency for carboxylic acids was also observed during the homogeneous electro-Fenton treatment of ENNXN (Fig. SM-1).

In the third step, determination of released inorganic ions was performed. The formations of fluoride, nitrate and ammonium were possible during the oxidation of ENNXN with hydroxyl radicals owing to the presence of heteroatoms (nitrogen and flour) in the structure. The chromatographic analysis with an ion-exchange column verified the presence of these ions (Fig. 12). A very fast accumulation rate was observed for all ions up to 90 min. After this time, the accu-

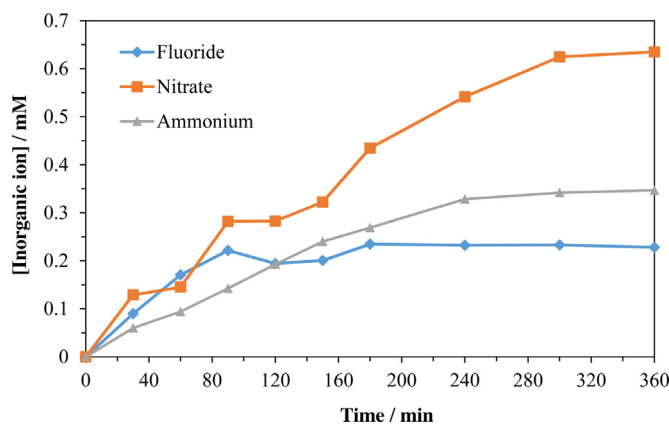


**Fig. 12.** The concentration-time profiles of released inorganic ions during the heterogeneous electro-Fenton treatment of ENXN.  $C_{ENXN}$ : 0.25 mM,  $[Na_2SO_4]$ : 0.01 M,  $m(Fe_2O_3-KLN)$ : 0.3 g, I: 60 mA, pH: 5.1, V: 0.175 L, T: 25 °C.

mulation rate of fluoride reached to its highest value (0.228 mM). This value corresponds to 92% of the initial amount of flour that found in ENXN structure. The remaining part of flour may be found in the structure of oxidation intermediates. Prominent amounts of nitrate (0.635 mM) and ammonium (0.346 mM) were accumulated in the reaction medium after 360 min electrolysis. The total amounts (0.981 mM) of nitrate and ammonium correspond to 98.1% of initial amounts ( $0.25 \text{ mM} \times 4 = 1.0 \text{ mM}$ ) of nitrogen atoms. The formation of these inorganic species was reported during homogeneous electro-Fenton treatment of ENXN [45]. On the other hand, they quantified only 29% of the initial nitrogen as ammonium and nitrate ions. According to these results, it can be concluded that the oxidation power of our heterogeneous electro-Fenton system is much higher than that of the reported study.

Identification and quantification of inorganic ions released during the homogeneous electro-Fenton treatment were also performed to compare the accumulation characteristics of inorganic ions (Fig. SM-2). A similar behaviour was observed in the accumulation characteristics of fluoride for both heterogeneous and homogeneous systems. On the other hand, accumulation of nitrate and ammonium showed different characteristics in the case of different systems. While the majority of the initial nitrogen was converted to ammonium in the homogeneous system, it was mainly converted to nitrate in the heterogeneous system. Though the exact reason not known, this difference may arise from the use of different pH values in homogeneous (3.0) and heterogeneous (5.1) systems.

### 3.6. Mineralization pathway of ENXN

To evaluate the dominant radicals that contribute the mineralization of ENXN, degradation behaviour of ENXN was investigated in the absence and presence of radical scavengers (TBA and BQ). The comparative degradation results were given in Fig. 13. Degradation rate of ENXN decreased prominently in the presence of TBA. This arises from the scavenging effect of TBA since TBA effectively scavenges all  $\bullet OH$  in solution produced from Eqs. (2) and (7) [34,46]. Similar results for the scavenging effects of TBA were reported during the electro-Fenton treatment of rhodamine B [46] and winery wastewater [34]. On the contrary to TBA, there was a very slight decrease in the degradation rate of ENXN in the presence of BQ, which is a  $\bullet O_2^-$  scavenger. This indicates that the formation of  $\bullet O_2^-$  is negligible in the studied experimental conditions. According to these results, it can be concluded that the degradation and mineralization of ENXN in the studied conditions mainly takes place by

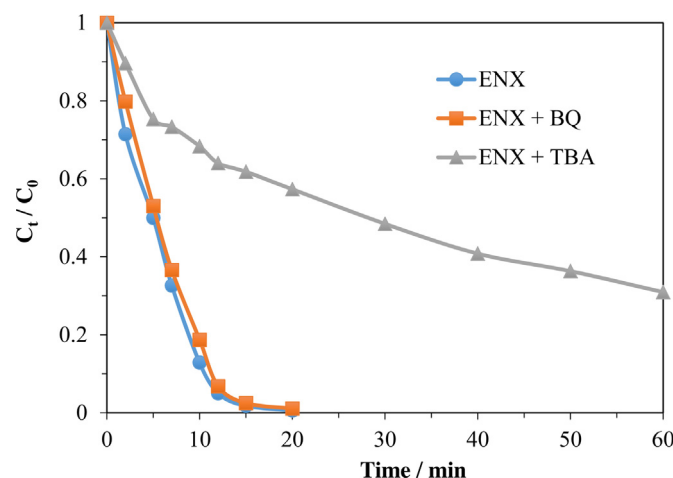


**Fig. 13.** Comparative degradation behaviours of 0.25 mM ENXN in the absence and presence of TBA or BQ during the heterogeneous electro-Fenton treatment. I: 60 mA, pH: 3.0,  $[Na_2SO_4]$ : 0.05 M,  $m(Fe_2O_3-KLN)$ : 0.3 g, V: 0.175 L, T: 25 °C.

the action of  $\bullet OH$  that formed from three sources (Eqs. (1), (2) and (7)).

A plausible oxidation route for the heterogeneous electro-Fenton removal of ENXN with  $Fe_2O_3$ -KLN catalyst was proposed based on the determined oxidation intermediates and assuming  $\bullet OH$  is the only oxidant in the system (Fig. 14). Oxidation of ENXN starts from two points; replacement flour atoms with hydroxyl group (II) and removal of carboxylic acid group from ENXN structure (III). The hydroxylation of II led to the formation of isomers IV and V. On the other hand, cleavage of piperazine ring also took place to form VI. Further reactions of these aromatic intermediates led to formation of short-chain aliphatic substances. These aliphatic substances except oxamic acid mainly converted to oxalic and formic acids. Finally, the mineralization of ENXN was completed by further oxidation of oxamic, oxalic and formic acids to form carbon dioxide, water and inorganic ions; fluoride, nitrate and ammonium.

## 4. Conclusions

Preparation and usage of an iron containing catalyst ( $Fe_2O_3$ -KLN) were investigated to obtain a heterogeneous electrocatalytic oxidation system. The proposed heterogeneous system was tested in the mineralization of ENXN. It was observed that ENXN removal rate was much higher in the presence of  $Fe_2O_3$ -KLN catalyst. The parameters that affect the efficiency of heterogeneous electro-Fenton treatment were investigated. The highest degradation and mineralization rates of ENXN were observed at 300 mA. While the efficiency of the system was significantly higher at low pH values (2 and 3), complete mineralization was also achieved at higher pH values (5.1 and 7.1). This eliminates pH adjustment during the electrolysis that is necessary for homogeneous systems. The prepared  $Fe_2O_3$ -KLN catalyst decreased the amount of waste iron sludge because the dissolved amount of iron from  $Fe_2O_3$ -KLN was very low ( $\sim 0.006 \text{ mM}$ ) according to the added amount (0.3 mM) of homogeneous  $Fe^{2+}$  catalyst. This is another significant advantage of the proposed system. Moreover,  $Fe_2O_3$ -KLN catalyst can be recovered by simple filtration process that enables the reuse of the catalyst. The degradation rate constant of ENXN in heterogeneous electro-Fenton conditions was determined as  $1.24 (\pm 0.04) \times 10^9 \text{ M}^{-1} \text{ s}^{-1}$ . Identification of oxidation intermediates of ENXN during the heterogeneous electro-Fenton treatment was performed by HPLC, GC-MS, LC-MS and IC analysis. Radical scavenging studies showed that  $\bullet OH$  is the main oxidant in the proposed heterogeneous electro-Fenton method. An oxidation pathway was

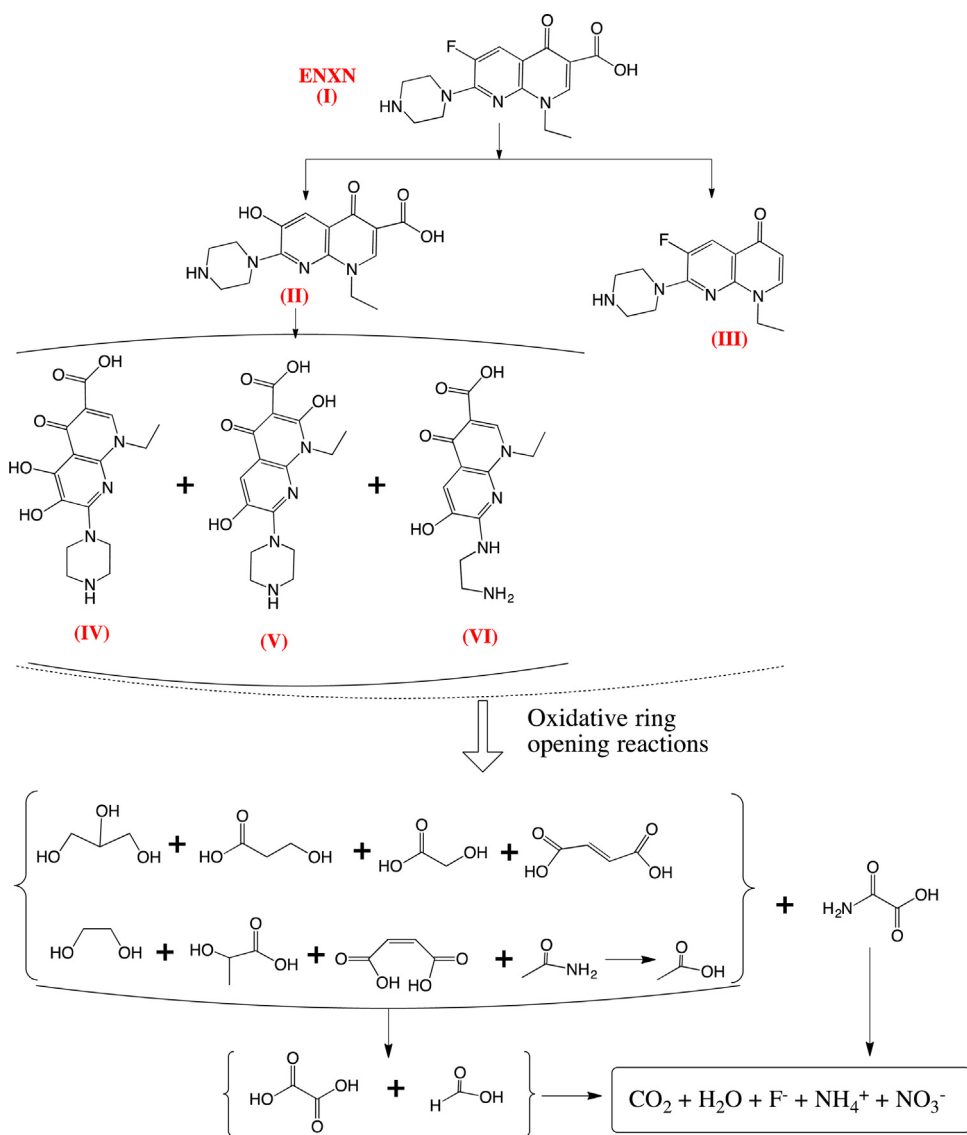


**Fig. 14.** Plausible oxidation routes for the mineralization of ENXN during the heterogeneous electro-Fenton treatment.

proposed based on the identified oxidation intermediates. Finally, it can be said that the use of  $\text{Fe}_2\text{O}_3$ -KLN catalyst in the heterogeneous electro-Fenton process increases the oxidation efficiency of organic pollutants and decreases the cost of the system.

## Acknowledgement

Financial support of Anadolu University Research Projects Commission (Project No: 1401F009) is gratefully acknowledged.

## Appendix A. Supplementary data

Supplementary data associated with this article can be found, in the online version, at <http://dx.doi.org/10.1016/j.apcatb.2016.07.018>.

## References

- [1] C.A. Martínez-Huitl, E. Brillas, *Appl. Catal. B: Environ.* 87 (2009) 105–145.
- [2] E. Brillas, I. Sirés, M.A. Oturan, *Chem. Rev.* 109 (2009) 6570–6631.
- [3] C. Flox, P.-L. Cabot, F. Centelles, J.A. Garrido, R.M. Rodríguez, C. Arias, E. Brillas, *Appl. Catal. B: Environ.* 75 (2007) 17–28.
- [4] M. Gençen, A. Özcan, *Chemosphere* 136 (2015) 167–173.
- [5] M.A. Oturan, N. Oturan, C. Lahitte, S. Trevin, *J. Electroanal. Chem.* 507 (2001) 96–102.
- [6] A. Özcan, Y. Şahin, A.S. Koparal, M.A. Oturan, *J. Hazard. Mater.* 153 (2008) 718–727.
- [7] A. Özcan, M.A. Oturan, N. Oturan, Y. Şahin, *J. Hazard. Mater.* 163 (2009) 1213–1220.
- [8] M. Pimentel, N. Oturan, M. Dezotti, M.A. Oturan, *Appl. Catal. B: Environ.* 83 (2008) 140–149.
- [9] F.C. Moreira, S. García-Segura, R.A.R. Boaventura, E. Brillas, V.J.P. Vilar, *Appl. Catal. B: Environ.* 160–161 (2014) 492–505.
- [10] A. Özcan, Y. Şahin, A.S. Koparal, M.A. Oturan, *Water Res.* 42 (2008) 2889–2898.
- [11] M.A. Oturan, N. Oturan, M.C. Edelahi, F.I. Podvorica, K. El Kacem, *J. Chem Eng.* 171 (2011) 127–135.
- [12] M.A. Oturan, E. Guivarch, N. Oturan, I. Sirés, *Appl. Catal. B: Environ.* 82 (2008) 244–254.
- [13] A. Özcan, Y. Şahin, M.A. Oturan, *Chemosphere* 73 (2008) 737–744.
- [14] M.S. Çelebi, N. Oturan, H. Zazou, M. Hamdani, M.A. Oturan, *Sep. Purif. Technol.* 156 (2015) 996–1002.
- [15] A. Dirany, I. Sirés, N. Oturan, A. Özcan, M.A. Oturan, *Environ. Sci. Technol.* 46 (2012) 4074–4082.
- [16] A. Özcan, Y. Şahin, A.S. Koparal, M.A. Oturan, *Appl. Catal. B: Environ.* 89 (2009) 620–626.
- [17] S.R. Popuri, C.Y. Chang, J. Xu, *Desalination* 277 (2011) 141–146.
- [18] S. Guo, G. Zhang, J. Wang, *J. Colloid Interface Sci.* 433 (2014) 1–8.
- [19] H. Hassan, B.H. Hameed, *J. Chem. Eng.* 171 (2011) 912–918.
- [20] C.M. Sánchez-Sánchez, E. Expósito, J. Casado, V. Montiel, *Electrochim. Commun.* 9 (2007) 19–24.
- [21] S. Ammar, M.A. Oturan, L. Labiad, A. Guersalli, R. Abdelhedi, N. Oturan, E. Brillas, *Water Res.* 74 (2015) 77–87.

- [22] N. Barhoumi, L. Labiad, M.A. Oturan, N. Oturan, A. Gadri, S. Ammar, E. Brillas, *Chemosphere* 141 (2015) 250–257.
- [23] L. Labiad, M.A. Oturan, M. Panizza, N. Ben Hamadi, S. Ammar, J. Hazard. Mater. 297 (2015) 34–41.
- [24] O. Iglesias, J. Gómez, M. Pazos, M.Á. Sanromán, *Appl. Catal. B: Environ.* 144 (2014) 416–424.
- [25] N.A. Zubir, C. Yacou, X. Zhang, J.C. Diniz da Costa, J. *Environ. Chem. Eng.* 2 (2014) 1881–1888.
- [26] W. He, Q. Ma, J. Wang, J. Yu, W. Bao, H. Ma, A. Amrane, *Appl. Clay Sci.* 99 (2014) 178–186.
- [27] N.K. Daud, B.H. Hameed, *Desalination* 269 (2011) 291–293.
- [28] H. Ma, Q. Zhuo, B. Wang, *J. Chem. Eng.* 155 (2009) 248–253.
- [29] X. Van Doorslaer, J. Dewulf, H. Van Langenhove, K. Demeestere, *Sci. Total Environ.* 500–501 (2014) 250–269.
- [30] J. Rivera-Utrilla, M. Sánchez-Polo, M.Á. Ferro-García, G. Prados-Joya, R. Ocampo-Pérez, *Chemosphere* 93 (2013) 1268–1287.
- [31] M.S. Yahya, N. Oturan, K. El Kacemi, M. El Karbane, C.T. Aravinda Kumar, M.A. Oturan, *Chemosphere* 117 (2014) 447–454.
- [32] V.S. Antonin, M.C. Santos, S. Garcia-Segura, E. Brillas, *Water Res.* 83 (2015) 31–41.
- [33] N. Barhoumi, N. Oturan, H. Olvera-Vargas, E. Brillas, A. Gadri, S. Ammar, M.A. Oturan, *Water Res.* 94 (2016) 52–61.
- [34] O. Iglesias, J. Mejide, E. Bocos, M.Á. Sanromán, M. Pazos, *Electrochim. Acta* 169 (2015) 134–141.
- [35] P.W. Hu, H.M. Yang, *Appl. Clay Sci.* 74 (2013) 58–65.
- [36] A. Özcan, Y. Şahin, M.A. Oturan, *Water Res.* 47 (2013) 1470–1479.
- [37] P.V. Nidheesh, R. Gandhimathi, *Desalination* 299 (2012) 1–15.
- [38] K. Kim, P. Qiu, M. Cui, J. Khim, *J. Chem. Eng.* 284 (2016) 1165–1173.
- [39] S. Loaiza-Ambuludi, M. Panizza, N. Oturan, A. Özcan, M.A. Oturan, J. *Electroanal. Chem.* 702 (2013) 31–36.
- [40] N. Oturan, J. Wu, H. Zhang, V.K. Sharma, M.A. Oturan, *Appl. Catal. B: Environ.* 140–141 (2013) 92–97.
- [41] K. Hanna, S. Chiron, M.A. Oturan, *Water Res.* 39 (2005) 2763–2773.
- [42] F.J. Beltrán, A. Aguinaco, J.F. García-Araya, *Water Res.* 43 (2009) 1359–1369.
- [43] L.R. Karam, D.S. Bergtold, M.G. Simic, *Free Radic. Res. Commun.* 12–13 (Pt. 1) (1991) 11–16.
- [44] G.V. Buxton, C.L. Greenstock, W.P. Helman, A.B. Ross, W. Tsang, *J. Phys. Chem. Ref. Data* 17 (1988) 513.
- [45] C. Annabi, F. Fourcade, I. Soutrel, F. Geneste, D. Floner, N. Bellakhal, A. Amrane, *J. Environ. Manage.* 165 (2016) 96–105.
- [46] W. Liu, Z. Ai, L. Zhang, J. Hazard. Mater. 243 (2012) 257–264.